

Compact self-gravitating solutions of quartic (K) fields in brane cosmology

C. Adam^{a*}, N. Grandi^{b**}, P. Klimas^{a***}, J. Sánchez-Guillén^{a†}, and A. Wereszczyński^{c††}

^{a)}Departamento de Física de Partículas, Universidad de Santiago
and Instituto Galego de Física de Altas Enerxías (IGFAE)

E-15782 Santiago de Compostela, Spain

^{b)}IFLP-CONICET

cc67 CP1900, La Plata, Argentina

^{c)}Institute of Physics, Jagiellonian University,
Reymonta 4, 30-059 Kraków, Poland

Abstract

Recently we proposed that K fields, that is, fields with a non-standard kinetic term, may provide a mechanism for the generation of thick branes, based on the following observations. Firstly, K field theories allow for soliton solutions with compact support, i.e., compactons. Compactons in 1+1 dimensions may give rise to topological defects of the domain wall type and with finite thickness in higher dimensions. Secondly, propagation of linear perturbations is confined inside the compacton domain wall. Further, these linear perturbations inside the topological defect are of the standard type, in spite of the non-standard kinetic term. Thirdly, when gravity is taken into account, location of gravity in the sense of Randall–Sundrum works for these compacton domain walls provided that the backreaction of gravity does not destabilize the compacton domain wall.

It is the purpose of the present paper to investigate in detail the existence and stability of compacton domain walls in the full K field and gravity system, using both analytical and numerical methods. We find that the existence of the domain wall in the full system requires a correlation between the gravitational constant and the bulk cosmological constant.

*adam@fpaxp1.usc.es

**grandi@fisica.unlp.edu.ar

***klimas.ftg@gmail.com

†joaquin@fpaxp1.usc.es

††wereszczynski@th.if.uj.edu.pl

1 Introduction

Recently, the idea that the visible universe with its 3+1 dimensions is embedded into some higher dimensional space has received considerable attention. Consistency with observations requires that the propagation of matter and fields is restricted to this 3+1 dimensional subspace, at least for not too high energies. In this context, two slightly different scenarios have been studied. The subspace may either be of the topological defect type, in which case it has a finite, although probably very small, extension in the additional dimensions. Some first proposals of this type have already been made in the eighties, see [1], [2]. In the last years, interest in this type of “topological defect” universes has increased significantly, and the name of “thick branes” has become customary for these objects. Some recent work may be found, e.g., in [3] - [7]. The other possibility is that the subspace is strictly 3+1 dimensional, in which case it is known as a “three-brane”. Investigation of these three-branes started in the nineties, and the literature on this subject is too numerous to be quoted here. Some recent reviews, in which also further references may be found, are, e.g., [8] - [10].

It is one of the crucial features of a “thick brane” cosmological model that a dynamical mechanism must exist which provides the confinement of all matter fields to the subspace. We recently proposed such a mechanism [11] which uses as its main ingredients a scalar field theory with a non-standard kinetic term (K field theory) and the observation that topological defects with a compact support (compactons) exist in this theory [12]. For different aspects of K field theory, we refer, e.g., to [13] - [20], whereas the theory of compactons is discussed, e.g., in [21] - [23]. Interestingly, the complete suppression of the propagation of fields outside the support of the compacton is an automatic result of the model proposed in [11]. Further, the propagation of linear perturbations inside the topological defect (i.e., inside the brane) is standard, in close similarity to the Kaluza–Klein reduction, in spite of the non-standard kinetic term. Specifically, there are no tachyons on the brane, and the evolution of linear perturbations is both unitary and causal. Inside the brane, the only remaining effect of the original K field theory resides in the values of the masses of the (Klein–Gordon type) linear fluctuation field.

For the full theory, with gravitation coupled minimally to the scalar field, we showed in the same paper that, provided the compacton domain wall is not destabilized by the addition of gravity, bulk gravity solutions of the Randall–Sundrum type [24] (that is, localization of gravity on the brane) do exist. However, the analysis of the stability of the full K field plus gravity system and specifically of the existence of the compacton domain walls in the full system was not done in Ref. [11]. It is the purpose of the present

paper to perform precisely this analysis.

In Section 2, we briefly present the model together with the resulting field equations and their vacuum solution. In Section 3 we present some analytic investigations of the system without gravity for later convenience. In Section 4 we turn to the analytic investigation of the full system with gravitation included. We perform a power series expansion about the boundary of the domain wall as well as about its center. Further, we establish some global properties of the resulting system of nonlinear evolution equations. The result of this analysis is that the compacton domain wall does not exist for completely generic values of the two remaining parameters (the gravitational coupling κ and the bulk cosmological constant Λ). Instead, the existence of the compacton requires a correlation between these two parameters, that is, for a given κ the compacton exists if Λ takes a fixed κ dependent value. In different words, the space of compacton solutions forms a one-dimensional curve in the κ - Λ plane. In Section 5 we turn to a numerical investigation of the full system. We determine the correlation between κ and Λ (i.e., the above mentioned line in the κ - Λ plane) to a high precision. Concretely, we fine-tune the value of κ for a given Λ . Further we determine the compacton radius, that is, the extension of the domain wall in the transverse direction. In addition, we display figures providing some details of the numerical investigation. In Section 6 we study the issue of stability of the compact domain walls established in the previous sections under linear fluctuations. Specifically, we prove by a combination of analytical and numerical methods that the domain wall is stable under fluctuations of the scalar K field also in the full theory, with gravitational backreaction included. Section 7 contains a discussion of our results.

2 The model

The action is (for details we refer to [11])

$$S = \int d^5x \sqrt{|g|} (\kappa^{-2}(R - \Lambda) + 4|X|X - V(\xi)) \quad (1)$$

where Λ is the cosmological constant, and X now includes the metric

$$X = \frac{1}{2} g^{MN} \partial_M \xi \partial_N \xi. \quad (2)$$

Further, the potential is

$$V(\xi) \equiv 3\lambda^4 (\xi^2 - a^2)^2, \quad (3)$$

We will choose a 5D metric ansatz with a Minkowskian 4D slice, written in the form

$$ds^2 = e^{-A(y)} (dt^2 - d\vec{x}^2) - dy^2. \quad (4)$$

We remind the reader that - up to coordinate transformations - this metric ansatz is the most general one having the Minkowski space symmetries ISO(3,1) on the brane, see e.g. [3]. For the scalar field we assume $\xi = \xi(y)$. Then the field equation for ξ is

$$-8A_y\xi_y^3 + 12\xi_y^2\xi_{yy} = 12\lambda^4\xi(\xi^2 - a^2) \quad (5)$$

and the independent components of the Einstein equations read

$$\frac{3}{4}A_{yy} - A_y^2 = \frac{1}{3} [\Lambda + \kappa^2 3\lambda^4(\xi^2 - a^2)^2] \quad (6)$$

$$\frac{3}{4}A_{yy} = \kappa^2\xi_y^4. \quad (7)$$

At first sight one might think that the system is overdetermined because there are three ODEs for the two unknown functions ξ and A , but the field equation for ξ is not independent of the Einstein equations. Indeed, when one calculates the y derivative of Eq. (6) and replaces A_{yy} and A_{yyy} with the help of Eq. (7), one recovers Eq. (5).

Remark: the derivation of the field equation for ξ from the Einstein equations requires a division by κ^2 and another division by ξ_y , therefore the field equation is a consequence of the Einstein equations provided that these two quantities are nonzero. In the vacuum sector, where $\xi_y = 0$, the field equation for ξ is more restrictive and requires that $\xi = \pm a$, whereas the Einstein equations would allow for more general constant values of ξ .

For later convenience, we rewrite the above system of equations in dimensionless quantities, by rescaling $\xi \rightarrow a\xi$, $V \rightarrow a^4V$, and $z = \lambda y$, $\lambda^{-1}\Lambda \rightarrow \Lambda$, $\lambda\kappa \rightarrow \kappa$. Further, we introduce the derivative $C(z) = A_z(z)$ as field variable, and get

$$-\frac{2}{3}C\xi_z^3 + \xi_z^2\xi_{zz} = \xi(\xi^2 - 1) \quad (8)$$

$$\frac{3}{4}C_z - C^2 = \frac{1}{3}\Lambda + \kappa^2(\xi^2 - 1)^2 \quad (9)$$

$$\frac{3}{4}C_z = \kappa^2\xi_z^4. \quad (10)$$

This system still has the vacuum solution

$$\xi = \pm 1 = \text{const.} \quad , \quad A = \sqrt{\frac{\Lambda}{3}}|z| + \text{const.} \quad \Rightarrow \quad C = \sqrt{\frac{\Lambda}{3}}\text{sign}(z) \quad (11)$$

where

$$\bar{\Lambda} \equiv -\Lambda \geq 0 \quad (12)$$

is a positive constant.

3 Non-gravitational case

The system without gravitation has the field equation

$$\xi_z^2 \xi_{zz} = \xi(\xi^2 - 1) \quad (13)$$

with the compacton solution

$$\xi(z) = \begin{cases} -1 & (z - z_0) \leq -\frac{\pi}{2} \\ \sin z & -\frac{\pi}{2} \leq (z - z_0) \leq \frac{\pi}{2} \\ 1 & (z - z_0) \geq \frac{\pi}{2}, \end{cases} \quad (14)$$

Here z_0 is the compacton center, which we shall frequently choose equal to $z_0 = 0$. Further, the compacton reaches the vacuum values $\xi = \pm 1$ at $z_{\pm} = z_0 \pm \frac{\pi}{2}$. We will use the notation z_0, z_{\pm} for the center and boundary of the compacton, respectively, also in the case with gravitation.

Although we know the explicit solution in the case without gravity, we want to study the behaviour of the solution near the lower boundary and the center for later convenience. We assume $z_0 = 0$ for the moment and introduce the new variable $t = z - z_- \equiv z + \frac{\pi}{2}$ (where $\xi(t = 0) \equiv \xi(z = z_-) = -1$ by assumption). The field equation remains unchanged,

$$\xi_t^2 \xi_{tt} = \xi(\xi^2 - 1) \quad (15)$$

because the translation $t = z - z_-$ is a symmetry. Now we insert the power series expansion

$$\xi = -1 + b_2 t^2 + b_3 t^3 + \dots \quad (16)$$

into the above equation (15) and find

$$8b_2^3 - 2b_2 = 0 \quad (17)$$

with the three solutions

$$b_2 = 0, \frac{1}{2}, -\frac{1}{2} \quad (18)$$

where $b_2 = 0$ corresponds to the vacuum solution and $b_2 = \frac{1}{2}$ corresponds to the compacton solution. $b_2 = -\frac{1}{2}$ corresponds to a solution growing in absolute value for increasing t , which has infinite energy and is of no interest

in this context. Observe, however, that $b_2 = -\frac{1}{2}$ together with $\xi(t=0) = 1$ would correspond to the anti-compacton. We remark that this degeneracy for the coefficient b_2 exists due to the nonlinearity in the kinetic term and would be absent in a theory with normal kinetic term. Once a choice for b_2 has been made, the higher coefficients b_n are determined uniquely by linear equations. For the choice $b_2 = \frac{1}{2}$, the higher coefficients just reproduce the power series of the function $\xi(t) = -\cos t$.

Next, we study the power series expansion about the compacton center $z_0 = 0$. By assumption, $\xi(z=0) = 0$, therefore the expansion is

$$\xi = b_1 z + b_2 z^2 + \dots \quad (19)$$

If we assume that $b_1 \neq 0$, then it automatically follows that all even b_n are zero, $b_{n=2m} = 0$. The odd b_n are determined by linear equations depending on the arbitrary nonzero b_1 . For the choice $b_1 = 1$ we recover the power series expansion of the function $\xi(z) = \sin z$. It is easy to see that finite energy requires, in fact, $b_1 = \pm 1$. Indeed, a first integration of the field equation gives

$$\xi_z^4 = (\xi^2 - 1)^2 + k \quad (20)$$

where k is an integration constant. Finite energy requires $k = 0$ which implies for $\xi(z_0) = 0$ that $\xi_z(z_0) = \pm 1$.

Finally, let us briefly recapitulate the necessary conditions for the existence of the compacton. These conditions are that

- 1) the field may be joined smoothly with smooth first derivative to its vacuum value. This holds because of the triple degeneracy of $b_2 = 0, \frac{1}{2}, -\frac{1}{2}$ at the compacton boundaries z_{\pm} .
- 2) the field, which starts at the value $\xi(z_-) = -1$ at z_- and obeys the compacton boundary condition $b_2 = \frac{1}{2}$, evolves such that it takes the value $\xi(z_0) = 0$ at some point z_0 . It may be checked easily that this property follows from the structure of the field equation.
- 3) the field resulting from the evolution of point 2) is odd about the point z_0 . This means that the evolution of ξ for $z > z_0$ will be the mirror image of the evolution for $z < z_0$ and, consequently, will join the other vacuum, $\xi = 1$, at $z_+ = 2z_0 - z_-$. This is automatically fulfilled in the case without gravitation, because a solution with initial condition $\xi(z_0) = 0, \xi_z(z_0) \neq 0$ is always an odd function about z_0 for arbitrary values of $\xi_z(z_0)$.

We remark that points 1) and 2) in the above list continue to hold in the case with gravitation. On the other hand, point 3) will not hold in the generic

case. Instead, it requires a fine-tuning between the gravitational coupling κ and the cosmological constant Λ .

4 The case with gravity

4.1 Expansion about the compacton boundary

We again introduce the variable $t = z - z_-$ where by assumption $\xi(z = z_-) = \xi(t = 0) = -1$, $\xi_t(t = 0) = 0$, and $C(t = 0) = -\sqrt{\bar{\Lambda}/3}$. The Einstein equations are

$$\frac{3}{4}C_t - C^2 = -\frac{1}{3}\bar{\Lambda} + \kappa^2(\xi^2 - 1)^2 \quad (21)$$

$$\frac{3}{4}C_t = \kappa^2\xi_t^4, \quad (22)$$

and we insert the power series expansion

$$\xi = -1 + b_2t^2 + b_3t^3 + b_4t^4 + \dots \quad (23)$$

$$C = -\sqrt{\bar{\Lambda}/3} + c_1t + c_2t^2 + \dots \quad (24)$$

For b_2 we find again Equation (17) with the three solutions (18), corresponding to vacuum, compacton and an infinite energy solution, respectively, like in the case without gravity. Choosing $b_2 = \frac{1}{2}$ for the compacton, the higher coefficients are, again, determined uniquely by linear equations. Concretely we find

$$b_3 = -\frac{1}{15}\sqrt{\frac{\bar{\Lambda}}{3}}, \quad b_5 = -\sqrt{\frac{\bar{\Lambda}}{3}}\frac{1}{420}\left(\frac{16\bar{\Lambda}}{75\cdot 3} + \frac{1}{2}\right) \quad (25)$$

$$b_4 = -\frac{1}{24} + \frac{1}{90}\frac{\bar{\Lambda}}{3}, \quad b_6 = \frac{223}{2\cdot 3^4\cdot 5^3\cdot 7}\left(\frac{\bar{\Lambda}}{3}\right)^2 + \frac{61}{2^4\cdot 3^3\cdot 5^2\cdot 7}\frac{\bar{\Lambda}}{3} + \frac{1}{720}. \quad (26)$$

These coefficients now depend on the cosmological constant and go to their nongravitational values (the expansion coefficients of $-\cos t$) in the limit $\bar{\Lambda} \rightarrow 0$, as they should. As b_3 is negative, the cosmological constant tends to increase the size of the compacton.

For the function C we find from Eq. (22) that the coefficients $c_1 - c_4$ are identically zero. The two first nontrivial coefficients are

$$c_5 = \frac{4\kappa^2}{15}, \quad c_6 = \frac{8}{45}\kappa^2\sqrt{\bar{\Lambda}/3}. \quad (27)$$

We remark that the first dependence of the b_i on the gravitational constant κ^2 enters for the coefficient b_8 . The effect of the gravitational backreaction on the power series expansion at the compacton boundary is, therefore, negligible for not too large values of the gravitational constant. The contribution of κ^2 to b_8 is positive, therefore the gravitational backreaction by itself tends to shrink the “compacton” radius.

4.2 Approximate determination of the compacton radius

The fact that the expansion coefficients almost do not depend on the gravitational constant κ^2 allows to determine the “compacton” radius $|z_0 - z_-|$ for a given cosmological constant Λ approximately. The idea is to use the power series expansion for $\xi(t)$ to a certain order, and to determine the first zero of this polynomial for $t > 0$. We warn that for a fixed Λ and arbitrary κ a true compacton does not exist. But the position of the first zero will almost not depend on κ , therefore this position should determine the compacton radius to a good approximation whenever the compacton exists, at least for not too large values of Λ and κ . Concretely, we will use the power series expansion up to sixth order, where κ does not show up at all.

Let us first check this proposal for the nongravitational case, where the exact compacton solution is known. This nongravitational solution is given in Eq. (14) therefore the compacton radius $\rho = |z_0 - z_-|$, variable t and function $\xi(t)$ are

$$\rho = \frac{\pi}{2}, \quad t = \frac{\pi}{2} + z, \quad \xi(t) = -\cos t \quad (28)$$

Observe that all even derivatives of $\xi(t)$ at the compacton center $t = \rho$ are zero, because ξ must be an odd function of $z = t - \rho$. Now we use the power series expansion of the function $\xi(t) = -\cos t$ about $t = 0$ up to sixth order to determine the zero ρ approximately, see Eq. (29).

$\xi(t)$	compacton radius ρ	$\xi''(t = z_0)$
exact $(-\cos t)$	$\pi/2 = 1.5708$	0
power series $(\mathcal{O}(t^6))$	1.5699	-0.0208

(29)

We find that the power series up to sixth order reproduces the exact value of the compacton radius to a precision of better than 10^{-3} . Further, we plot the value of the second derivative at the compacton center, $\xi''(t = \rho)$, which must be zero for the exact solution. This value is off about 2% for the approximation.

cosmological constant $\bar{\Lambda}$	compacton radius ρ
0	1.5699
0.0001	1.57145
0.001	1.57481
0.0025	1.57767
0.005	1.58092
0.01	1.58554
0.025	1.59488
0.05	1.6058
0.1	1.62233

Table 1: Approximate determination of the compacton radius from the power series expansion

Now we do the same calculation for the power series up to sixth order using the coefficients b_i of the previous subsection for the case with gravitation and cosmological constant included, for different values of the cosmological constant. The result is presented in Table 1. It is clearly seen that the compacton radius increases with the cosmological constant. Later we shall compare these simple results with a numerical integration and will find that, indeed, they reproduce the compacton radius with a rather good precision. We repeat that the existence of the compacton requires a fine-tuning of the value of κ , but that the value of the ‘‘compacton radius’’ calculated above is completely insensitive to the value of κ .

4.3 Expansion about the center

Now we want to study a power series expansion about z_0 where by definition $\xi(z = z_0) = 0$. Here we use the Einstein equations in the slightly rewritten form

$$C_z = \frac{4}{3} \left(C^2 + \kappa^2 (\xi^2 - 1)^2 - \frac{\bar{\Lambda}}{3} \right) \quad (30)$$

$$\xi_z = \frac{1}{\sqrt{\kappa}} \left(C^2 + \kappa^2 (\xi^2 - 1)^2 - \frac{\bar{\Lambda}}{3} \right)^{\frac{1}{4}} \quad (31)$$

where we choose the positive root for ξ_z , which describes the compacton (the negative root would give the antcompacton). As said, for a compacton $\xi(z)$ must be an odd function about z_0 . It may be checked easily that a necessary

and sufficient condition for this is that C is equal to zero at z_0 , too, $C(z_0) = 0$. Therefore, the conditions at the center of a compacton are

$$\xi(z_0) = 0 \quad , \quad C(z_0) = 0. \quad (32)$$

These equations already demonstrate the possible troubles for the existence of a compacton. For suppose we start the evolution at the lower compacton boundary $\xi(z_-) = -1$, $C(z_-) = -\sqrt{\bar{\Lambda}/3}$ and for compacton boundary conditions (i.e. $b_2 = 1/2$). After some evolution $\xi(z)$ will hit a point z_0 such that $\xi(z_0) = 0$, but there is no reason that $C(z)$ has evolved to the same value $C(z_0) = 0$ at $z = z_0$. The condition $C(z_0) = 0$ is an additional condition for the already completely determined initial value problem (evolution from the compacton boundary with compacton boundary conditions) and requires, therefore, a fine-tuning of the parameters κ and $\bar{\Lambda}$.

A first conclusion which may be drawn easily is that $\bar{\Lambda} > 0$ for $\kappa \neq 0$ is a necessary condition for the existence of a compacton. For assume that we start the evolution of the fields at the center with conditions $\xi(z_0) = 0$, $C(z_0) = 0$ for $\bar{\Lambda} = 0$. The evolution equations are

$$C_z = \frac{4}{3} (C^2 + \kappa^2(\xi^2 - 1)^2) \quad (33)$$

$$\xi_z = \frac{1}{\sqrt{\kappa}} (C^2 + \kappa^2(\xi^2 - 1)^2)^{\frac{1}{4}}. \quad (34)$$

From these equations and the conditions $C(z_0) = 0$, $C_z(z_0) > 0$ it follows that $C(z)$ is strictly positive for $z > z_0$, and from this it follows in turn that both C_z and ξ_z are strictly positive for all $z > z_0$. Therefore, ξ can never reach a point z_+ where $\xi_z(z_+) = 0$, which is the compacton boundary condition at the upper boundary of the compacton. The conclusion is that a compacton cannot exist for $\kappa \neq 0$ and $\bar{\Lambda} = 0$.

An upper bound can be easily found for $\bar{\Lambda}$ by inserting the power series expansion

$$\xi = b_1 z + b_3 z^3 + \dots \quad (35)$$

$$C = c_1 z + c_3 z^3 + \dots \quad (36)$$

into the above evolution equations (we assume momentarily that $z_0 = 0$). It immediately follows that

$$b_1 = \frac{1}{\sqrt{\kappa}} \left(\kappa^2 - \frac{\bar{\Lambda}}{3} \right)^{\frac{1}{4}} \quad (37)$$

which is real only provided that

$$\bar{\Lambda} \leq 3\kappa^2. \quad (38)$$

Some further qualitative conclusions may be drawn by investigating the evolution equations (30), (31), by assuming an evolution from the center z_0 . The problem is that ξ_z must reach its value zero exactly at the same point z_+ where ξ takes the value +1. When ξ_z has not yet reached zero at the point z_+ where $\xi(z_+) = +1$, then it will never reach zero, because from this point onward both quantities C^2 and $(\xi^2 - 1)^2$ start to grow. This happens for too small $\bar{\Lambda}$ for a given κ . On the other hand, if ξ_z takes its value zero before ξ reaches the value one, then all the higher derivatives of ξ at this point are singular, and the evolution equations break down at this point. This happens when $\bar{\Lambda}$ is too big for a given κ . Therefore, for each given $\kappa \neq 0$, there exists precisely one fine tuned value of $\bar{\Lambda}$ such that ξ_z is zero exactly at the point z_+ where ξ takes the value +1, and, consequently, the compacton exists only for this fine-tuned value.

Remark: One may derive a single first order evolution equations for the “orbit” $C(\xi)$, and this equation may be used to determine the correlation between $\bar{\Lambda}$ and κ (but not for the compacton radius). Indeed, dividing (30) by (31) one easily derives the following equation,

$$\tilde{C}_\xi = \beta \left[\tilde{C}^2 - 1 + \alpha(\xi^2 - 1)^2 \right]^{\frac{3}{4}} \quad (39)$$

where

$$\tilde{C} \equiv \sqrt{\frac{3}{\bar{\Lambda}}} C, \quad \alpha \equiv \frac{3\kappa^2}{\bar{\Lambda}}, \quad \beta \equiv \frac{4}{3} \left(\frac{\kappa^2 \bar{\Lambda}}{3} \right)^{\frac{1}{4}}. \quad (40)$$

Between the compacton center and the upper compacton boundary (or, indeed, between the lower and upper compacton boundary) both C_z and ξ_z are strictly monotonous, therefore this “orbit” equation indeed may describe the compacton. Integrating, e.g., from the center of the compacton to the upper boundary requires the “initial” condition (at the center) $\tilde{C}(\xi = 0) = 0$ and the condition $\tilde{C}(\xi = 1) = 1$. These two conditions for a first order ODE overdetermine the system and do not have a solution in general. Closer inspection of the above equation (39) again reveals that there exists exactly one β for given α (or one α for given β) such that the compacton exists. Indeed, as \tilde{C}_ξ always grows with growing α for fixed β (and always grows with growing β for fixed α), independently of the values of \tilde{C} and ξ , the above statement follows. The numerical values of α and β (and, therefore, of $\bar{\Lambda}$ and κ) such that the compacton exists may be easily determined numerically from Eq. (39) and completely agree with the values determined from the numerical solution of the system of equations (30) and (31) presented in Table 2 and Fig. 1. We present the result of a numerical integration for some fine-tuned values of κ and $\bar{\Lambda}$ in the last figure (Fig. 15). Indeed, for these

fine-tuned values the function $\tilde{C}(\xi)$ reaches the value one at $\xi = 1$ to a high precision.

5 Numerical calculations

Here we present the numerical calculations for the Einstein equations (9), (10). First we display the results for the fine-tuned values of κ for a given $\bar{\Lambda}$, as well as the corresponding compacton radius, see Figures 1, 2 and Table 2. The fine-tuned value of κ for a given $\bar{\Lambda}$ is defined by the condition that the numerical integration reproduces the compacton configuration. When κ is too big (or, equivalently, $\bar{\Lambda}$ is too small), then ξ_z will never reach the value zero. When κ is too small (or, equivalently, $\bar{\Lambda}$ is too big), then ξ_z reaches zero before ξ reaches one. At this point a singularity forms and the numerical integration breaks down. The fine-tuned value for κ is just the boundary case between these two cases. More precisely, the values for κ^2 in Figure 1 and Table 2 are determined from a numerical integration which starts at the center of the “compacton”, that is, with initial values $C = 0$, $\xi = 0$ (“shooting from the center”). Within this numerical intergration, the displayed values for κ^2 are the smallest values for κ^2 that can be found numerically such that a singularity does not form in the numerical integration. Strictly speaking, they are, therefore, upper bounds for the true fine-tuned values of κ^2 , but they are determined to a high precision.

In Table 2, we provide two values for the compacton radius. The first, ρ_c , is determined by a shooting from the center, like κ^2 itself. The advantage of this value is that it provides a strict lower bound on the compacton radius, because the “compacton” radius strictly decreases with increasing κ^2 for a shooting from the center (here the “compacton” radius is defined as the point z_+ where $\xi(z_+) = 1$, which is at the same time the point where ξ_z has a local minimum), and the used value for κ^2 is an upper bound. The disadvantage of ρ_c is that its value is extremely sensitive to a precise determination of κ^2 . An error in the seventh of eighth digit for κ^2 , for instance, frequently translates into an error in the third digit for ρ_c . Therefore, we determine the compacton radius in Table 2 also from a numerical integration which starts at the lower boundary of the compacton with compacton boundary conditions (“shooting from the lower boundary”). We know already from the power series analysis of the last section that the so determined “compacton” radius ρ_b almost does not depend on the exact value of κ^2 (here the “compacton” radius is defined as the point $t = z_0$ where $\xi(t = z_0) = 0$). Therefore, we expect the so

$\bar{\Lambda}$	κ^2	ρ_c	ρ_b
10^{-8}	0.000073512465	1.56782	1.57096
10^{-6}	0.00073531885	1.56817	1.57105
10^{-5}	0.00232675114	1.57047	1.57127
10^{-4}	0.00737252306	1.57080	1.57195
0.001	0.0234612031	1.57251	1.57412
0.005	0.0530591779	1.57515	1.57804
0.01	0.0756746147	1.57896	1.58097
0.025	0.1216666085	1.58443	1.59200
0.05	0.1753053396	1.58917	1.59852
0.1	0.2544852246	1.59367	1.60259
0.2	0.3732506647	1.60912	1.61565
0.3	0.4698973846	1.62347	1.62565
0.5	0.6332261243	1.63673	1.64145
0.7	0.7752995199	1.65032	1.65425
1.0	0.9666302322	1.66660	1.67030
1.5	1.252723578	1.68682	1.69224
2.0	1.514998322	1.70648	1.71058
3.0	1.999550771	1.73613	1.74101
5.0	2.886273449	1.78229	1.78828

Table 2: Numerical determination of the fine-tuned value for κ^2 and of the corresponding compacton radius. The displayed value of κ^2 for a given $\bar{\Lambda}$ is the lowest value of κ^2 that can be found numerically by a shooting from the center, such that a singularity does not form in the numerical integration. Therefore, the true value of κ^2 could be slightly smaller, and the value in the table is, in fact, an upper bound. Correspondingly, the value of the compacton radius ρ_c , which is also determined by a shooting from the center, is a lower bound. The values for κ^2 are shown to a very high precision (with many digits), because the determination of ρ_c depends very sensitively on a precise determination of κ . Finally, we display the compacton radius ρ_b which is determined by a shooting from the boundary and depends on κ^2 only very weakly.

determined value ρ_b to better reproduce the true compacton radius than ρ_c . We find, for instance, that ρ_b obeys $\rho_b > (\pi/2)$ for all $\bar{\Lambda}$, which we know must be true at least for small $\bar{\Lambda}$ (see the power series expansion analysis of the last section). The disadvantage of ρ_b is that it no longer provides a strict lower bound, therefore we display both values.

Next, we present figures with some details from the numerical integration. We do the numerical integration in two different ways. First, we start at the center where both ξ and C are zero (“shooting from the center”), see Figures 3-8. We fix $\bar{\Lambda} = 0.5$ and choose for κ the fine-tuned value as well as one slightly smaller and one slightly bigger value. The results for other values of $\bar{\Lambda}$ are completely equivalent, and we choose the value of 0.5 for $\bar{\Lambda}$ just for convenience.

Then, we present the corresponding figures which one obtains for the numerical integration which starts at the lower boundary of the compacton (more precisely, very near the lower boundary, where the compacton boundary condition $b_2 = 1/2$ is taken into account), and integrates all the way up to the upper boundary (“shooting from the lower boundary”), see Figures 9-14. We remark that from these figures one may see explicitly that the “compacton radius” ρ_b determined from the shooting from the lower boundary depends only weakly on κ^2 , and therefore, approximates the true compacton radius rather well even if κ^2 is not exactly equal to its fine-tuned value. Indeed, from Figures 9, 11, and 13 we find the following values for ρ_b , given $\bar{\Lambda} = 0.5$ and the values for κ^2 indicated in the table,

$\bar{\Lambda}$	κ^2	ρ_b
0.5	0.633226	1.64145
0.5	0.608400	1.64236
0.5	0.640000	1.64121

(41)

where the first value $\kappa^2 = 0.633226$ is the fine-tuned value. We find that when κ^2 has a relative deviation of about 10^{-2} from its fine-tuned value, then the relative deviation of ρ_b is about $2 \cdot 10^{-5}$, i.e., quite small, indeed.

Finally, we present the result of a numerical integration of the “orbit” equation (39) for some fine-tuned values of κ and $\bar{\Lambda}$, with initial condition $\tilde{C}(\xi = 0) = 0$. For the fine-tuned values \tilde{C} reaches the value $\tilde{C}(\xi = 1) = 1$ to a high precision.

We conclude that the numerical analysis completely confirms the qualitative discussion of the last section, both for an evolution from the center and an evolution from the boundary of the compacton.

6 Linear Stability

In this section we want to discuss the issue of stability of the compacton domain wall under linear fluctuations. We shall not further comment on the issue of stability under gravitational fluctuations. Stability under fluctuations of the gravitational field for a whole class of thick brane models has been extensively discussed in Ref. [3], and we demonstrated already in Ref. [11] that our compact domain wall solutions belong to that class and, therefore, the analysis of Ref. [3] applies.

On the other hand, we want to study linear stability under fluctuations of the scalar field for the system with gravitational backreaction (for the compacton without gravity, linear stability has already been demonstrated in Ref. [11]). It turns out that stability of the full system with gravity may indeed be demonstrated by a combination of analytical and numerical methods, at least for not too large values of $\bar{\Lambda}$ (and, consequently, also for not too large values of κ). The restriction to not too large values of $\bar{\Lambda}$ probably does not mean that stability does not hold for large values, but just indicates that an approximation used in our proof becomes too crude for large values of $\bar{\Lambda}$.

The linear fluctuation equation for the scalar field is

$$\xi_z^2 \eta_{zz} + 2(\xi_z \xi_{zz} - A_z \xi_z^2) \eta_z - (3\xi^2 - 1)\eta = \frac{1}{3} e^A \xi_z^2 \square \eta \quad (42)$$

where \square is the four-dimensional Minkowski space wave operator, and A and ξ are the compact brane solutions of Sections 4, 5. Further, η is the linear fluctuation. Outside the compacton region, where the fields ξ and A take their vacuum values (specifically, $\xi_z = 0$), the only possible solution is $\eta = 0$, like in the non-gravitational case. For the case inside the compacton region, we use the separation of variable ansatz $\eta \rightarrow \eta(z)\phi(x)$ and get

$$\square \phi = -\omega^2 \phi \quad (43)$$

(the Klein–Gordon equation) and

$$\eta_{zz} + 2\left(\frac{\xi_{zz}}{\xi_z} - A_z\right)\eta_z - \frac{3\xi^2 - 1}{\xi_z^2}\eta = -\omega^2 e^A \eta \quad (44)$$

where ω^2 is the separation constant. After the transformation $\eta = \frac{e^A}{\xi_z} \bar{\eta}$, Equation (44) can be brought into the Schroedinger equation form

$$-\bar{\eta}_{zz} + U(z)\bar{\eta} = \omega^2 e^A \bar{\eta} \quad (45)$$

where

$$U(z) \equiv A_z^2 - A_{zz} + \frac{\xi_{zzz}}{\xi_z} - 2A_z \frac{\xi_{zz}}{\xi_z} + \frac{3\xi^2 - 1}{\xi_z^2}. \quad (46)$$

We now eliminate all higher derivatives terms (first and higher derivatives of ξ , second derivative of A) with the help of the field equations for ξ and A . Further, we again use the notation $C(z) \equiv A_z$, $C = \frac{\bar{\Lambda}}{3}\bar{C}$ and find

$$\begin{aligned} U = & -\frac{4}{9}\Gamma + \frac{\bar{\Lambda}}{27}\bar{C}^2 + \frac{8}{3}\kappa^{\frac{3}{2}}\sqrt{\frac{\bar{\Lambda}}{3}}\bar{C}\xi\frac{1-\xi^2}{\sqrt{\Gamma}}\Gamma^{-\frac{1}{4}} - \\ & - 2\kappa\frac{1-\xi^2}{\sqrt{\Gamma}} + 4\kappa\xi^2\Gamma^{-\frac{1}{2}} - 2\kappa^3\frac{(1-\xi^2)^2}{\Gamma}\xi^2\Gamma^{-\frac{1}{2}} \end{aligned} \quad (47)$$

where

$$\Gamma = \frac{\bar{\Lambda}}{3}(\bar{C}^2 - 1) + \kappa^2(\xi^2 - 1)^2. \quad (48)$$

Stability requires $\omega^2 \geq 0$. This, in turn, follows from the positive semi-definiteness of the above Schroedinger operator

$$H \equiv -\partial_z^2 + U \quad (49)$$

because from $\langle \eta | H | \eta \rangle \geq 0$ and the obvious $\langle \eta | e^A | \eta \rangle > 0$ it follows that $\omega^2 \geq 0$.

Next, let us study some properties of the potential U . U tends to plus infinity at the compacton boundaries $z = \pm\rho$ (here we assume that the compacton center is at $z = 0$). This follows from the fact that Γ goes to zero at the compacton boundaries, and from the fact that

$$\lim_{z \rightarrow \pm\rho} \frac{(1-\xi^2)^2}{\Gamma} = \kappa^{-2}$$

Further, U takes its only minimum at the center $z = 0$, where $\xi(z = 0) = 0$ and $C(z = 0) = 0$. The value at the minimum is

$$U_0 \equiv U(z = 0) = -\frac{4}{9}\left(\kappa^2 - \frac{\bar{\Lambda}}{3}\right) - \frac{2\kappa}{(\kappa^2 - \frac{\bar{\Lambda}}{3})^{\frac{1}{2}}} \quad (50)$$

The fact that U has an extremum at the center follows from the symmetry of U under the reflection $z \rightarrow -z$, whereas the fact that this is the only extremum (minimum) of U is not so easy to prove, because both the compacton solutions ξ and C and the correlation between $\bar{\Lambda}$ and κ are needed to demonstrate it. Here we restrict ourselves to a numerical demonstration. The potential U is plotted for the three values $\bar{\Lambda} = 10^{-3}, 0.5, 6.0$ in Figure 16. The behaviour described above is clearly seen in these figures. It follows that

the Schroedinger operator with potential U has a discrete, non-degenerate spectrum of eigenvalues

$$H\psi_n = E_n\psi_n \quad , \quad E_1 < E_2 < E_3 < \dots \quad (51)$$

and we want to demonstrate that $E_1 = 0$, $E_n > 0$ for $n = 2, 3, \dots$. Observe that we have to expect one zero eigenvalue because of the Goldstone mode of the translational symmetry $z \rightarrow z + a$.

The idea now is to find a new potential \bar{U} which is less or equal to the potential U for all z in the compacton region,

$$\bar{U}(z) \leq U(z) \quad , \quad z \in [-\rho, \rho] \quad (52)$$

and to study the spectral problem

$$\bar{H}\bar{\psi}_n \equiv (-\partial_z^2 + \bar{U})\bar{\psi}_n = \bar{E}_n\bar{\psi}_n \quad , \quad \bar{E}_1 < \bar{E}_2 < \bar{E}_3 < \dots \quad (53)$$

for this new potential \bar{U} . Stability is proved if the new potential has precisely one negative eigenvalue \bar{E}_1 , whereas all the other eigenvalues $\bar{E}_n, n \geq 2$ are positive. This follows from the inequality (which we prove below, see Eq. (59))

$$E_n \geq \bar{E}_n \quad \forall \quad n \quad (54)$$

because then $E_2 \geq \bar{E}_2 > 0$ and, consequently, only the lowest eigenvalue E_1 can be less or equal to zero. Finally, we know that it must be equal to zero, $E_1 = 0$, because we know that a zero eigenvalue must exist (the above-mentioned Goldstone mode of the translational symmetry $z \rightarrow z + a$). Therefore, the Schroedinger operator H cannot have a negative eigenvalue, which is what we wanted to prove.

Concretely, we choose the infinite square well potential for \bar{U} , which is plus infinity at the compacton boundaries, and equal to U_0 in the interior. The spectrum for this potential is well-known and is given by the eigenvalues

$$\bar{E}_n = \frac{\pi^2 \hbar^2}{2mL^2} n^2 + U_0 \quad (55)$$

where L is the width of the square well. In our case $\frac{\hbar^2}{2m} = 1$ and $L = 2\rho$ and, therefore,

$$\bar{E}_n = \frac{\pi^2}{4\rho^2} n^2 + U_0. \quad (56)$$

Stability requires $\bar{E}_1 < 0$ and $\bar{E}_2 > 0$ or

$$\bar{E}_1 \equiv \frac{\pi^2}{4\rho^2} + U_0 < 0 \quad (57)$$

$$\bar{E}_2 \equiv \frac{\pi^2}{\rho^2} + U_0 > 0 \quad (58)$$

where U_0 is given in Eq. (50) and for ρ , $\bar{\Lambda}$ and κ the values of Table 2 have to be used.

Qualitatively we can observe at once from Table 2 that our stability proof cannot work for arbitrarily large $\bar{\Lambda}$, because $|U_0|$ grows with growing $\bar{\Lambda}$, whereas ρ^{-2} shrinks with growing $\bar{\Lambda}$. The numerical results are shown in Figure 17 (for \bar{E}_1) and in Figure 18 (for \bar{E}_2). We find that $\bar{E}_1 < 0$ for all $\bar{\Lambda}$ as must hold because of the existence of the Goldstone mode. For \bar{E}_2 we find that $\bar{E}_2 > 0$ at least for $0 \leq \bar{\Lambda} \leq 2$, therefore we have proved stability for this parameter region.

Remark: we could, in principle, determine the value of $\bar{\Lambda}$ where the transition from positive to negative \bar{E}_2 occurs with higher precision (it will happen very near to $\bar{\Lambda} = 3$). But this would require the numerical solution of the compacton-gravity system for these values of $\bar{\Lambda}$, which is quite demanding and does not produce important new insights, therefore we do not perform this calculation here.

Remark: the fact that our stability proof does not work for high values of $\bar{\Lambda}$ does not necessarily mean that stability does not hold for these high values. It could just be the case that the approximation of the true potential U by the infinite square well \bar{U} is worse for higher values of $\bar{\Lambda}$. This is indeed indicated by the potentials U plotted in Figure 16. The higher the value of $\bar{\Lambda}$, the steeper the valley in the center of the potential, and the worse the approximation by a flat line.

Remark: the stability proof also works in the limit $\bar{\Lambda} \rightarrow 0$, $\kappa \rightarrow 0$, that is, in the non-gravitational case. This may be seen most directly by using the non-gravitational compacton solution $\rho = \frac{\pi}{2}$, $\xi = \sin z$ and the resulting potential $U = -2 + 2 \tan^2 z$, which obviously may be bound by an infinite square wall potential with depth $U_0 = -2$. Therefore, our stability proof also provides an alternative proof for the stability of the non-gravitational compacton of Ref. [12], [11].

Finally, we still have to prove the inequality (54) which we used in our stability proof. The proof only uses elementary quantum mechanics, but as we could not find it in any of the standard text books, we provide it here for completeness.

Theorem: Given the two Schroedinger operators $H = -\partial_z^2 + U(z)$ and $\bar{H} = -\partial_z^2 + \bar{U}(z)$ where $U(z) \geq U_0 \forall z \in (-\rho, \rho)$, $\bar{U}(z) \geq \bar{U}_0 \forall z \in (-\rho, \rho)$, $\lim_{z \rightarrow \pm\rho} U(z) = +\infty$ and $\lim_{z \rightarrow \pm\rho} \bar{U}(z) = +\infty$ such that the spectrum of both H and \bar{H} is purely discrete and non-degenerate,

$$\begin{aligned} H\psi_n &= E_n\psi_n \quad , \quad E_1 < E_2 < E_3 < \dots \\ \bar{H}\bar{\psi}_n &= \bar{E}_n\bar{\psi}_n \quad , \quad \bar{E}_1 < \bar{E}_2 < \bar{E}_3 < \dots \end{aligned}$$

and further it holds that

$$U(z) \geq \bar{U}(z) \quad \forall \quad z \in (-\rho, \rho)$$

then the inequality

$$E_n \geq \bar{E}_n \quad \forall \quad n$$

holds.

Proof: We define the Schroedinger operator

$$H(s) \equiv -\partial_z^2 + \bar{U} + s(U - \bar{U}) \quad (59)$$

which has a purely discrete and non-degenerate spectrum

$$H(s)\psi_n(s) = E_n(s)\psi_n(s) \quad (60)$$

for all $s \in [0, 1]$. It follows that

$$E_n(s) = \langle \psi_n(s) | H(s) | \psi_n(s) \rangle \quad (61)$$

and, after a derivative w.r.t. s , and using that

$$\langle (d/ds)\psi_n(s) | \psi_n(s) \rangle + \langle \psi_n(s) | (d/ds)\psi_n(s) \rangle = 0,$$

we further get

$$\frac{d}{ds}E_n(s) = \langle \psi_n(s) | (U - \bar{U}) | \psi_n(s) \rangle \geq 0, \quad (62)$$

from which the theorem follows immediately. QED.

7 Discussion

In this paper, we completed the investigation which we started in [11], studying in detail the existence of compact domain wall solutions in the full system of a quartic K field coupled to gravity. The result of this investigation is that such compact domain walls do exist, but their existence requires a correlation between the gravitational coupling κ and the bulk cosmological constant Λ . Further, these compact domain walls are stable under linear perturbations. Firstly, we want to emphasize that the correlation between the gravitational coupling κ and the bulk cosmological constant Λ we find in our system is qualitatively different from a fine-tuning which is frequently found in three-brane models. There, a fine-tuning between the bulk cosmological constant and the brane tension (or some related parameters of the brane) is necessary in order

to achieve a vanishing effective four-dimensional cosmological constant. In our case, on the other hand, the full action density is always zero on-shell locally (i.e., for any local solution of the Einstein equations). The correlation is needed, instead, to guarantee the global existence of a solution with finite energy in the transverse direction in the non-gravitational sector alone, that is, the global existence of a topological defect or domain wall. This correlation is, in fact, a rather interesting observation by itself. One may see it as a drawback, requiring a “fine-tuning” of the cosmological constant for a given gravitational constant, or as an advantage, providing a “prediction” of the bulk cosmological constant from the value of the gravitational constant and the requirement of the existence of a thick brane universe. Quantitatively, the diameter of the brane in the transverse direction grows with growing cosmological constant, and this growth may be seen as the net result of two competing influences. The gravitational constant by itself tends to shrink the brane size, whereas the cosmological constant tends to increase it. But these two constants are correlated, and the influence of the cosmological constant is stronger. The net effect is, therefore, an increase in the size of the brane.

Another interesting point consists in the fact that we were able to go rather far in the analysis of the model, establishing both the existence and the stability of the compact domain wall solutions, as well as its numerical properties to a high precision. Due to the inherent nonlinearity of the gravitational backreaction, such systems are usually quite difficult to analyse, and some simplifying assumptions (like replacing the “matter” fields by some effective energy momentum distribution) are frequently employed. In the present paper, on the other hand, we performed a full field theory calculation without any of these simplifying assumptions.

Further, let us emphasize that the results of this paper should be easily generalizable to other models. In fact, all that is needed is the presence of a potential term for the scalar K field which allows for a vacuum degeneracy, and the presence of a generalized kinetic term which takes a certain non-standard form in the limit of low energy. Still, this latter condition is rather nontrivial, because the absence of the standard quadratic kinetic term at low energies is a necessary condition. In this sense these models are special, because the presence of the quadratic term is a typical feature of low energy effective theories. Under which conditions these special theories may be induced remains an open problem at the moment, which deserves further study. In any case, the fact that essential features of brane physics, like domain walls of compact support, suppression of linear propagation outside the domain wall, and standard linear propagation inside the brane, are naturally provided by these models, makes it worth studying these special theories.

Finally, we want to mention that recently K field theories have been used

within the context of brane physics for a slightly different purpose in [25]. In that paper it was shown that the distance between different (thin) branes may be stabilized if the bulk scalar field has a nonstandard kinetic term.

Acknowledgements

C.A., P.K. and J.S.-G. thank MCyT (Spain) and FEDER (FPA2005-01963), and support from Xunta de Galicia (grant PGIDIT06PXIB296182PR and Conselleria de Educacion). A.W. acknowledges support from the Foundation for Polish Science FNP (KOLUMB programme) and Ministry of Science and Higher Education of Poland (grant N N202 126735). N.E.G. thanks Xunta de Galicia for support and Departamento de Fisica de Particulas - Universidade de Santiago de Compostela for hospitality during this work. Further, the authors thank O. Alvarez for helpful correspondence related to the stability proof of Section 6.

References

- [1] K. Akama, "Pregeometry" in: Lecture Notes in Physics, 176, Gauge Theory and Gravitation, Proceedings, Nara, 1982, ed. K. Kikkawa, N. Nakanishi and H. Nariai, 267-271 (Springer-Verlag,1983), hep-th/0001113.
- [2] V.A. Rubakov and M.E. Shaposhnikov, Phys. Lett. B125 (1983) 136
- [3] C. Csaki, J. Erlich, T.J. Hollowood, Y. Shirman, Nucl. Phys. B581 (2000) 309, hep-th/0001033.
- [4] R. Emparan, R. Gregory, C. Santos, Phys. Rev. D63 (2001) 104022, hep-th/0012100.
- [5] S. Kobayashi, K. Koyama , J. Soda, Phys. Rev. D65 (2002) 064014, hep-th/0107025.
- [6] K.A. Bronnikov , B.E. Meierovich, Grav. Cosmol. 9 (2003) 313, gr-qc/0402030.
- [7] A.A. Andrianov, L. Vecchi, arXiv:0711.1955.
- [8] D. Langlois, Prog. Theor. Phys. Suppl. 148 (2003) 181, hep-th/0209261.
- [9] F. Quevedo, Class. Quant. Grav. 19 (2002) 5721, hep-th/0210292.

- [10] P. Brax, C. van de Bruck, *Class. Quant. Grav.* 20 (2003) R201, hep-th/0303095.
- [11] C. Adam, N. Grandi, J. Sánchez-Guillén and A. Wereszczyński, *J. Phys. A*41 (2008) 212004, arXiv:0711.3550.
- [12] C. Adam, J. Sánchez-Guillén and A. Wereszczyński, *J. Phys. A*40 (2007) 13625, arXiv:0705.3554.
- [13] C. Armendariz-Picon, T. Damour, V.F. Mukhanov, *Phys. Lett. B*458 (1999) 209, hep-th/9904075.
- [14] J. Garriga, V.F. Mukhanov, *Phys. Lett. B*458 (1999) 219, hep-th/9904176.
- [15] T. Chiba, T. Okabe, M. Yamaguchi, *Phys. Rev. D*62 (2000) 023511, astro-ph/9912463.
- [16] C. Armendariz-Picon, V.F. Mukhanov, P.J. Steinhardt, *Phys. Rev. Lett.* 85 (2000) 4438, astro-ph/0004134.
- [17] C. Armendariz-Picon, V.F. Mukhanov, P.J. Steinhardt, *Phys. Rev. D*63 (2001) 103510, astro-ph/0006373.
- [18] E. Babichev, V.F. Mukhanov and A. Vikman, arXiv:0708.0561.
- [19] E. Babichev, *Phys. Rev. D*74 (2006) 085004, hep-th/0608071
- [20] B. Bazeia, L. Losano, R. Menezes, and J.C.R.E. Oliveira, *Eur. Phys. J. C* 51 (2007) 953, hep-th/0702052.
- [21] H. Arodz, *Acta Phys. Polon.* B33 (2002) 1241, nlin/0201001.
- [22] H. Arodz, P. Klimas, T. Tyranowski, *Acta Phys. Polon.* B36 (2005) 3861, hep-th/0510204
- [23] H. Arodz, P. Klimas, T. Tyranowski, *Acta Phys. Polon.* B38 3099 (2007), hep-th/0701148
- [24] L. Randall, R. Sundrum, *Phys. Rev. Lett.* 83 (1999) 4690, hep-th/9906064.
- [25] M. Olechowski, arXiv:0801.1605 [hep-th].

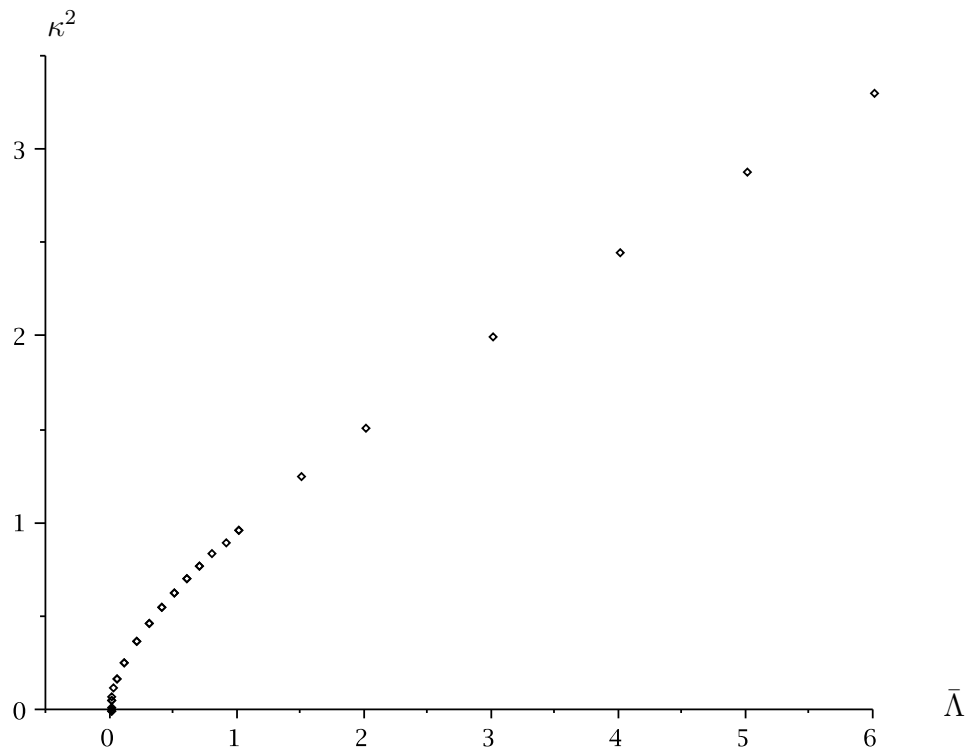


Figure 1: The fine-tuned values of κ and $\bar{\Lambda}$, for which a compacton exists, in the $\bar{\Lambda}$ - κ^2 plane, for some selected values.

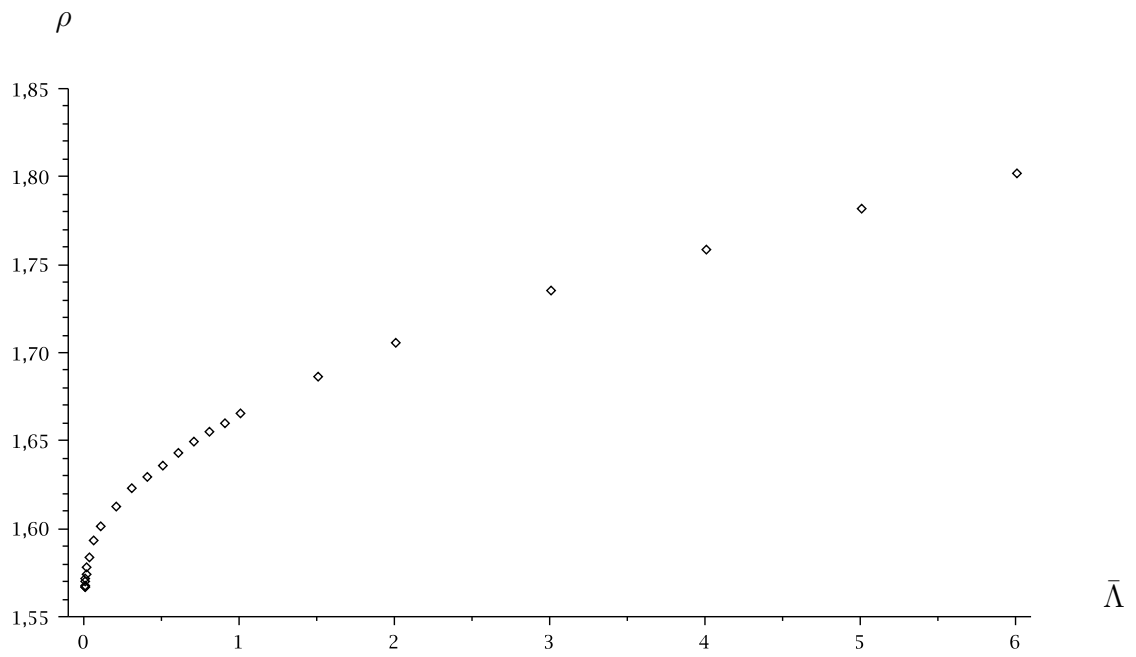


Figure 2: The compacton radius ρ for some selected values of $\bar{\Lambda}$ (and for the corresponding fine-tuned values of κ^2 such that the compacton exists), in the $\bar{\Lambda}$ - ρ plane.

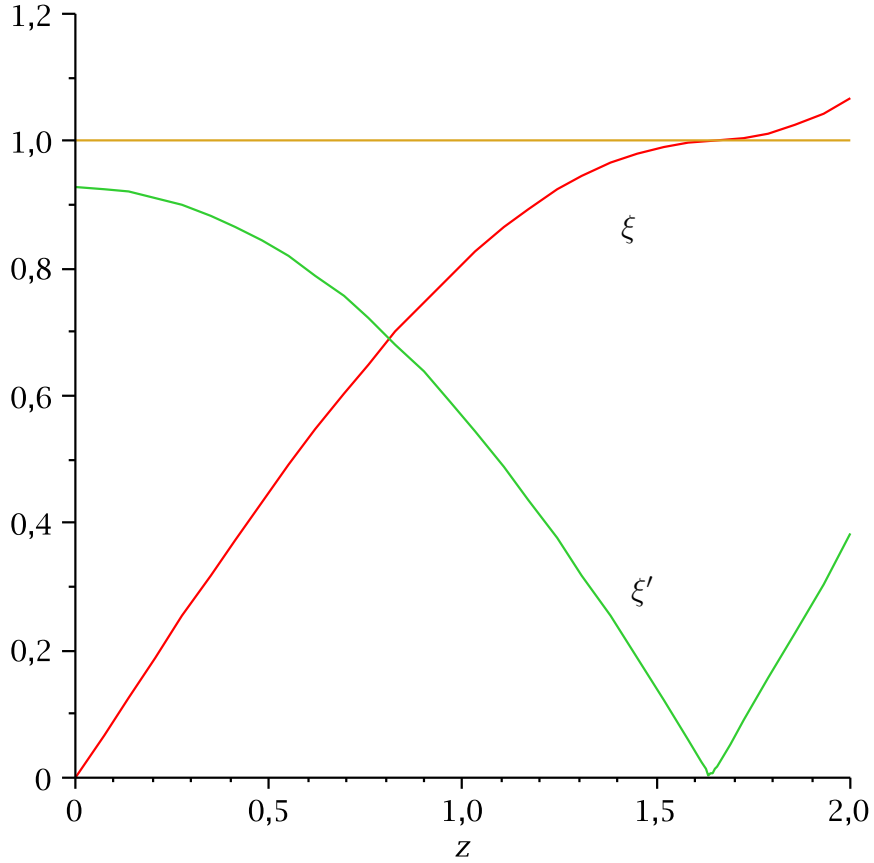


Figure 3: Shooting from the center: for $\bar{\Lambda} = 0.5$ and for the fine-tuned value $\kappa^2 = 0.633226$ the functions ξ and $\xi' \equiv \xi_z$ are shown. The compacton field ξ takes its vacuum value $\xi = 1$ exactly at the point where $\xi_z = 0$ (the compacton boundary). To the right of the compacton boundary the numerical integration selects the compacton configuration instead of the (correct) vacuum configuration, because numerically ξ_z never is exactly zero (because in that case the numerical integration would break down).

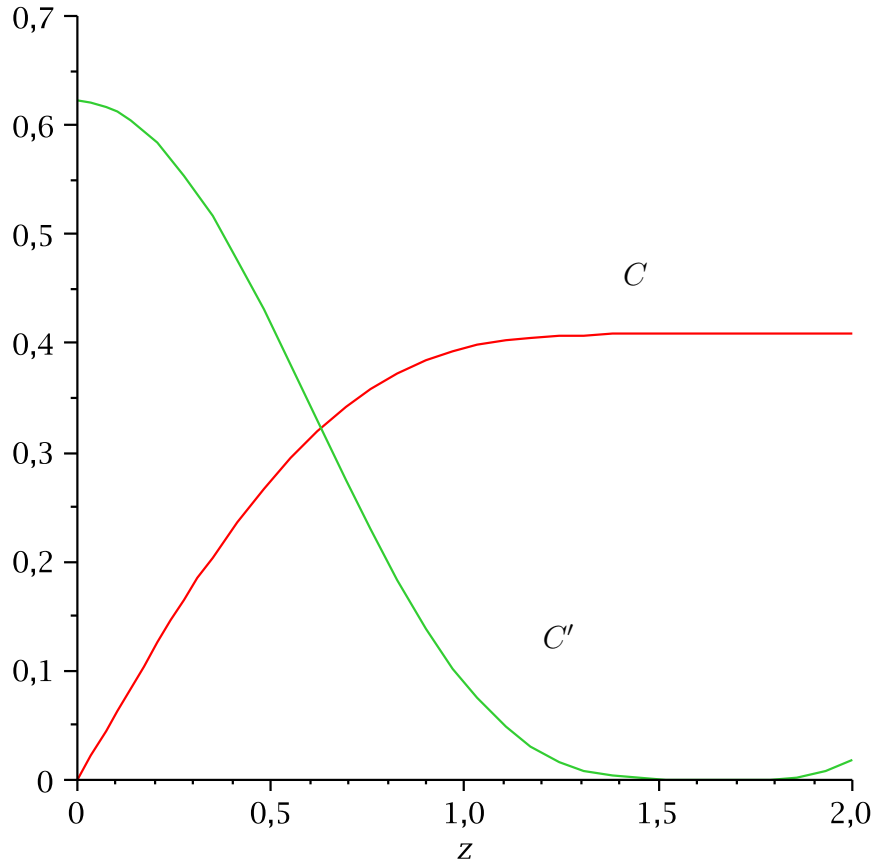


Figure 4: Shooting from the center: for $\bar{\Lambda} = 0.5$ and for the fine-tuned value $\kappa^2 = 0.633226$ (the same values as in Figure 3) the functions C and $C' \equiv C_z$ are shown. The field C takes its vacuum value $C = \sqrt{\bar{\Lambda}/3}$ exactly at the point where $\xi_z = C_z = 0$ (the compacton boundary). The curve is very flat near the compacton boundary, because the first four derivatives of C at the boundary are zero. To the right of the compacton boundary the numerical integration selects the compacton configuration instead of the (correct) vacuum configuration, for the same reason as in Figure 3.

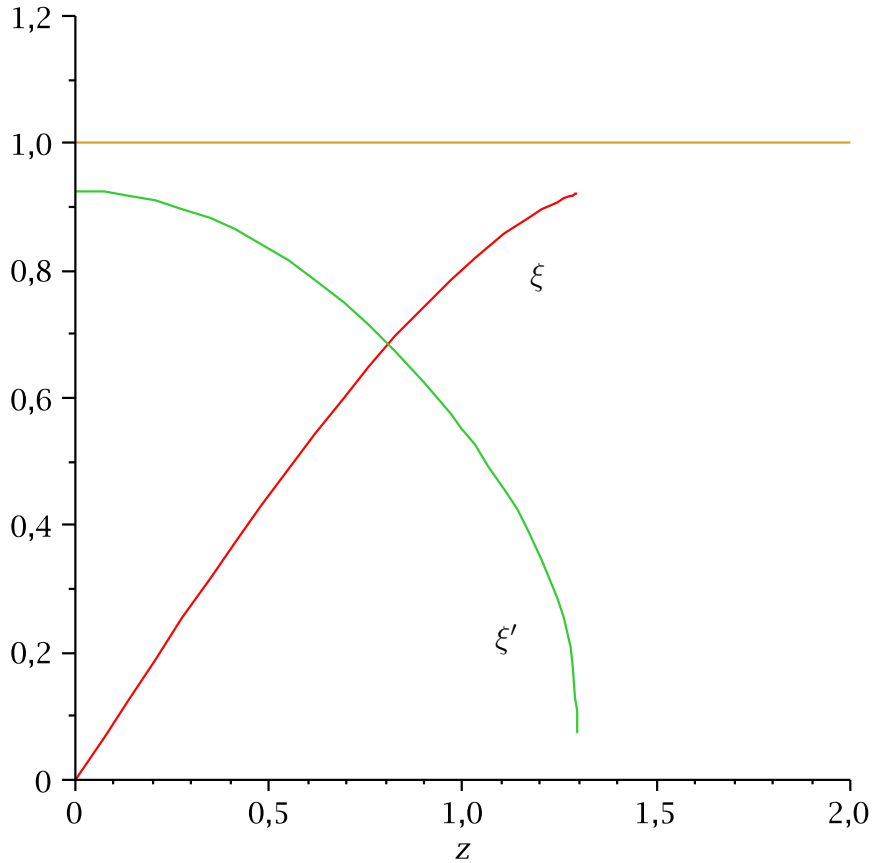


Figure 5: Shooting from the center: for $\bar{\Lambda} = 0.5$ and for $\kappa^2 = 0.621335$ (slightly smaller than the fine-tuned value) the functions ξ and $\xi' \equiv \xi_z$ are shown. The field ξ' reaches the value $\xi' = 0$ before ξ reaches its vacuum value $\xi = 1$. Further, all higher derivatives of ξ become singular at that point. Therefore, the numerical integration breaks down at this point. The numerical value of the point where the integration breaks down is $z = 1.29653$.

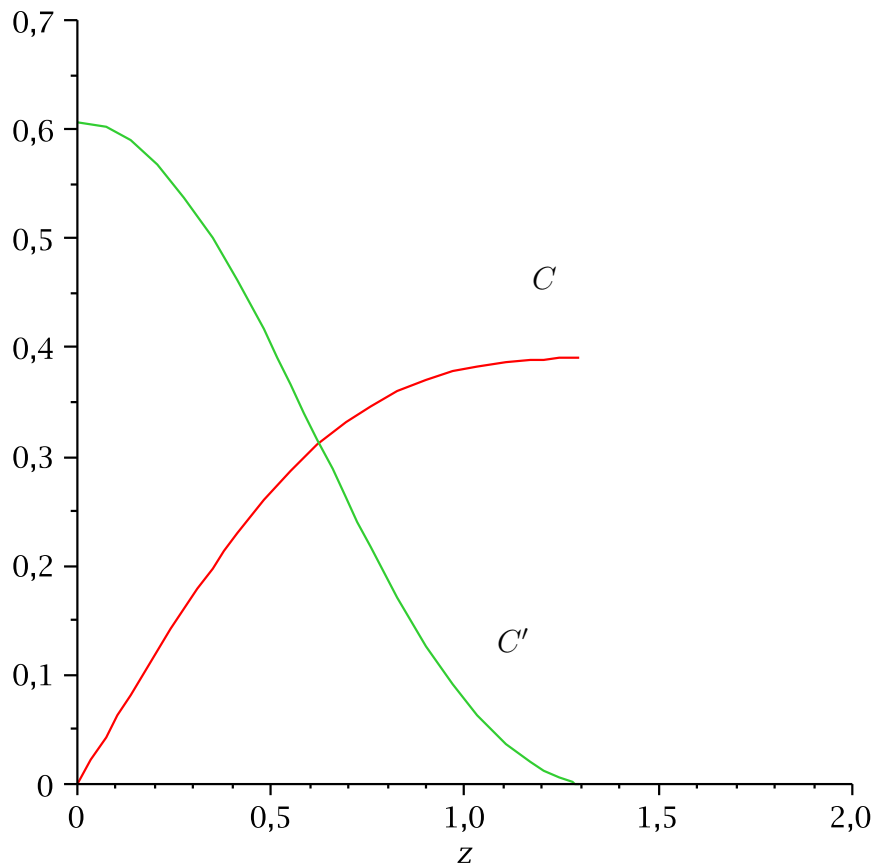


Figure 6: Shooting from the center: for $\bar{\Lambda} = 0.5$ and $\kappa^2 = 0.621335$ (slightly smaller than the fine-tuned value), like in Figure 4, the functions C and $C' \equiv C_z$ are shown. The field C' reaches the value $C' = 0$ before ξ and C reach their vacuum values. The numerical integration breaks down at this point because of the singularity in the integration for ξ , like in Figure 5.

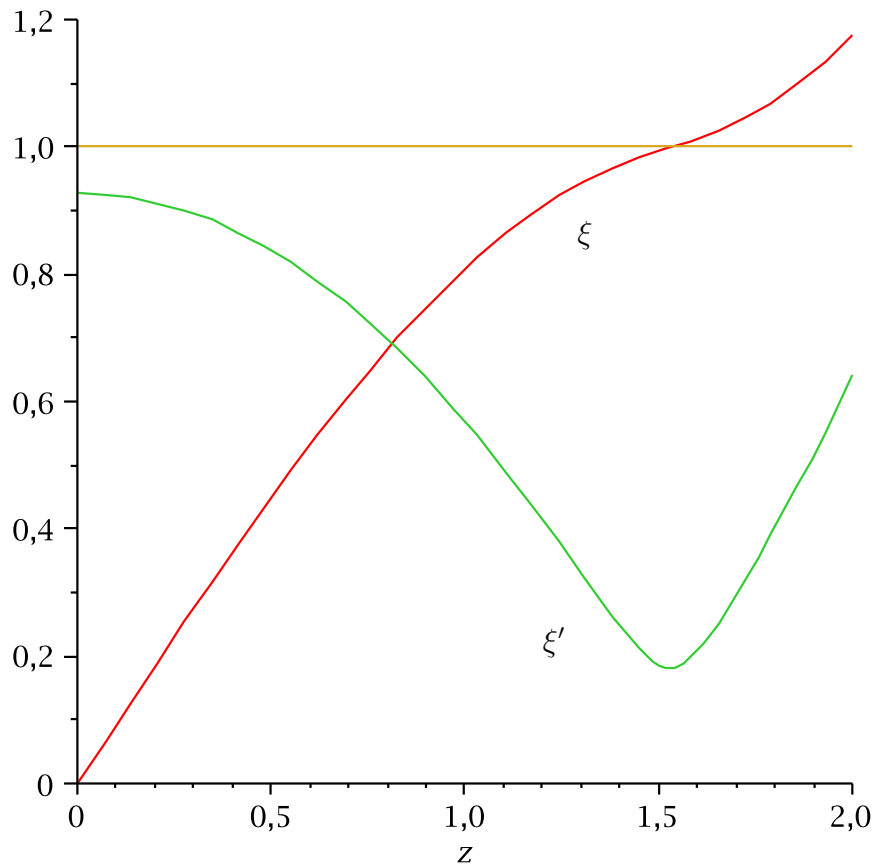


Figure 7: Shooting from the center: for $\bar{\Lambda} = 0.5$ and for $\kappa^2 = 0.633693$ (slightly bigger than the fine-tuned value) the functions ξ and $\xi' \equiv \xi_z$ are shown. The field ξ' never reaches the value $\xi' = 0$, therefore the field ξ never settles down at its vacuum value.

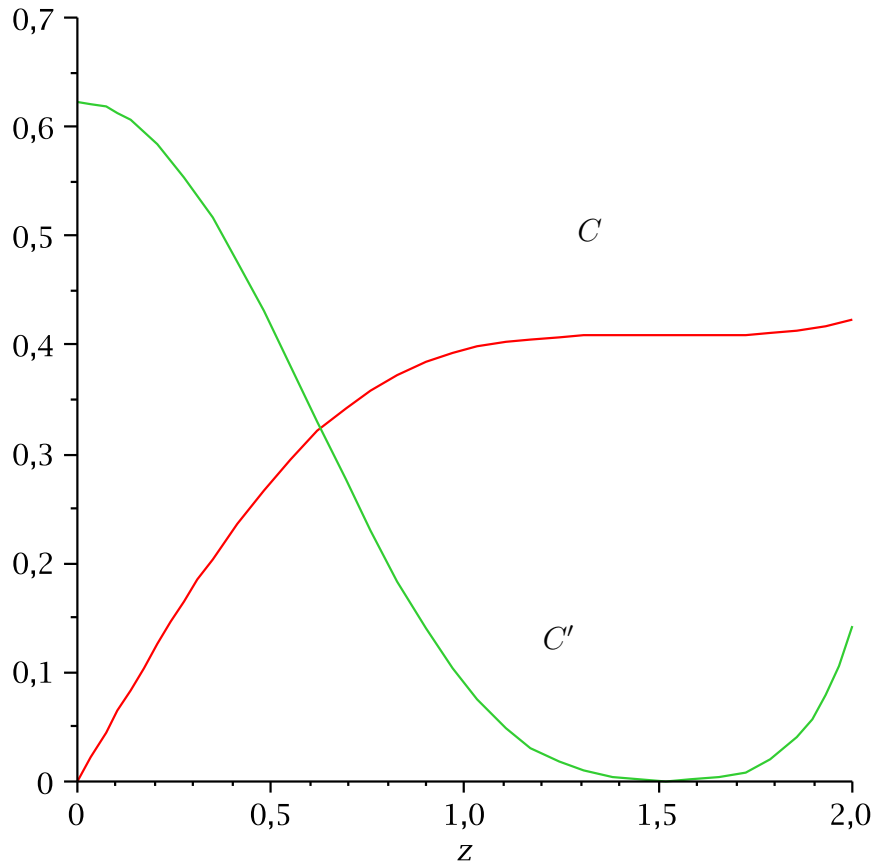


Figure 8: Shooting from the center: for $\bar{\Lambda} = 0.5$ and for $\kappa^2 = 0.633693$ (slightly bigger than the fine-tuned value), like in Figure 7, the functions C and $C' \equiv C_z$ are shown. The field C never settles down at its vacuum value (the fact that C' does not reach zero is not obvious from the figure, because it takes very small values numerically near the region where $\xi \sim 1$. But it may be checked easily by direct numerical calculation, or by amplifying that region in the figure).

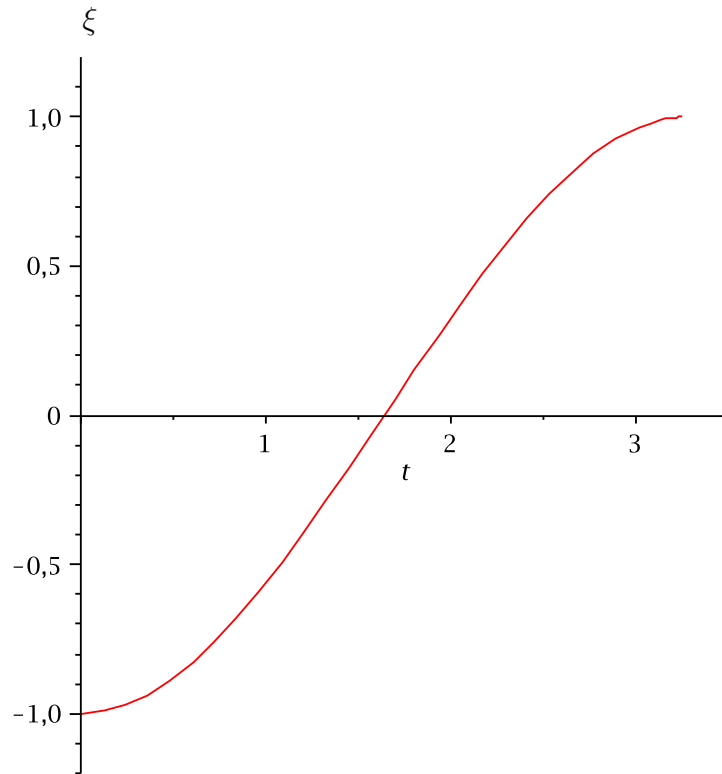


Figure 9: Shooting from the lower boundary: for $\bar{\Lambda} = 0.5$ and for the fine-tuned value $\kappa^2 = 0.633226$, like in Figure 3, the function ξ is shown. The compacton field ξ takes its opposite vacuum value $\xi = +1$ exactly at the point where $\xi_z = 0$ again (the upper compacton boundary). The graph of the function ξ is exactly odd about the compacton center (where $\xi = 0$). This compacton center $t = z_0$ is at $z_0 = 1.6414529$

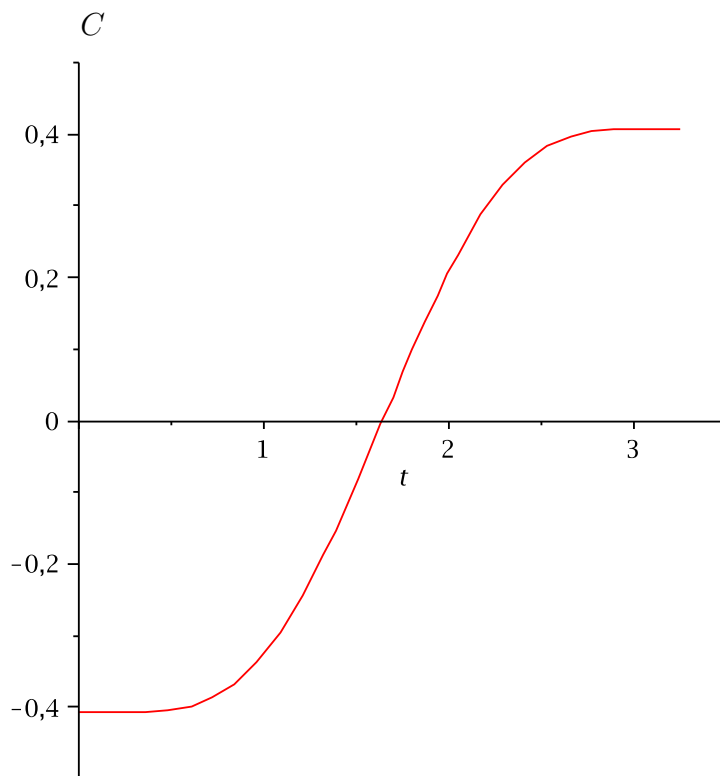


Figure 10: Shooting from the lower boundary: for $\bar{\Lambda} = 0.5$ and for the fine-tuned value $\kappa^2 = 0.633226$ (the same values as in Figure 3) the function C is shown. The field C takes its opposite vacuum value $C = +\sqrt{\bar{\Lambda}/3}$ exactly at the point where $\xi_z = C_z = 0$ again (the upper compacton boundary). The curve is very flat near the compacton boundaries, because the first four derivatives of C at the boundaries are zero. The graph of the function C is exactly odd about the compacton center (where $\xi = C = 0$). Numerically, this center is at $t = 1.6414542$, which agrees with the compacton center for ξ in Figure 9 in the first six digits.

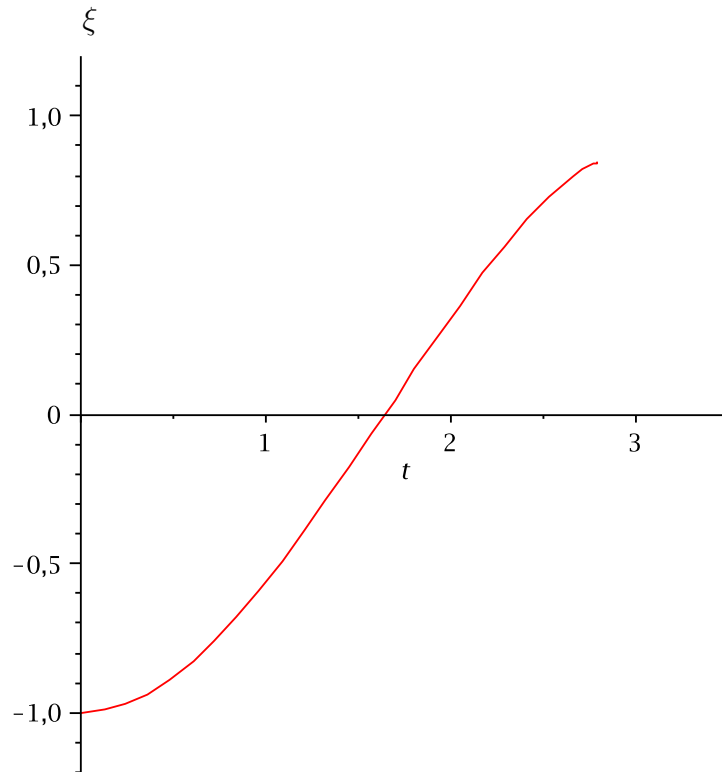


Figure 11: Shooting from the lower boundary: for $\bar{\Lambda} = 0.5$ and for $\kappa^2 = 0.608400$ (slightly smaller than the fine-tuned value), the function ξ is shown. The field ξ' reaches the value $\xi' = 0$ before ξ reaches its vacuum value $\xi = 1$. Therefore, the numerical integration breaks down at this point. The numerical value of the point where the integration breaks down is $t = 2.79688$. The numerical value of the “compacton center” where $\xi(t) = 0$ is $t = 1.64236$.

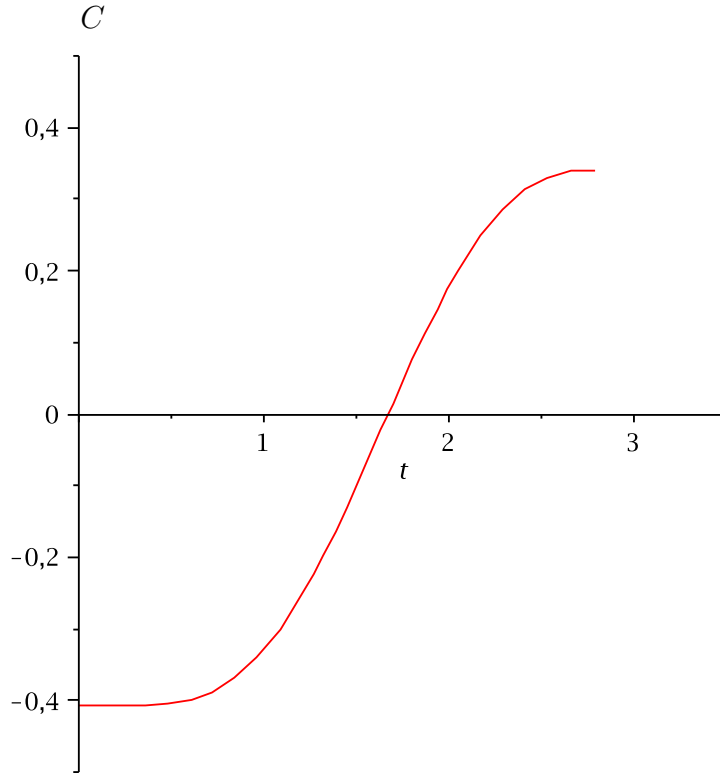


Figure 12: Shooting from the lower boundary: for $\bar{\Lambda} = 0.5$ and $\kappa^2 = 0.608400$ (slightly smaller than the fine-tuned value), the function C is shown. The field C' reaches the value $C' = 0$ before ξ and C reach their vacuum values. The numerical integration breaks down at this point because of the singularity in the integration for ξ , like in Figure 11. The field $C(t)$ takes the value zero at $t = 1.67201$, which is markedly different from the point where the field ξ takes the value zero in Figure 11.

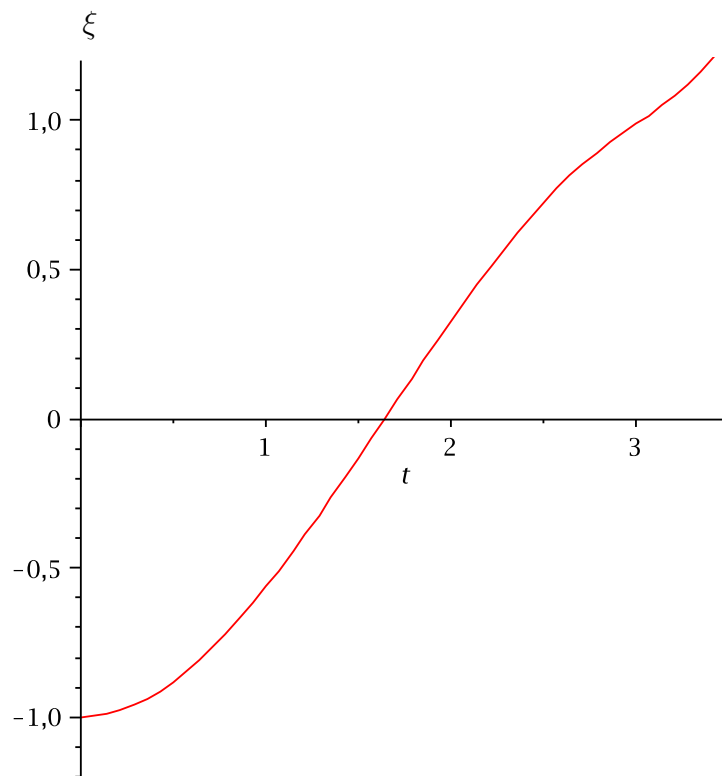


Figure 13: Shooting from the lower boundary: for $\bar{\Lambda} = 0.5$ and for $\kappa^2 = 0.640000$ (slightly bigger than the fine-tuned value), the function ξ is shown. The field ξ' never reaches the value $\xi' = 0$, therefore the field ξ never settles down at its vacuum value. The point where $\xi(t) = 0$ is at $t = 1.641214$.

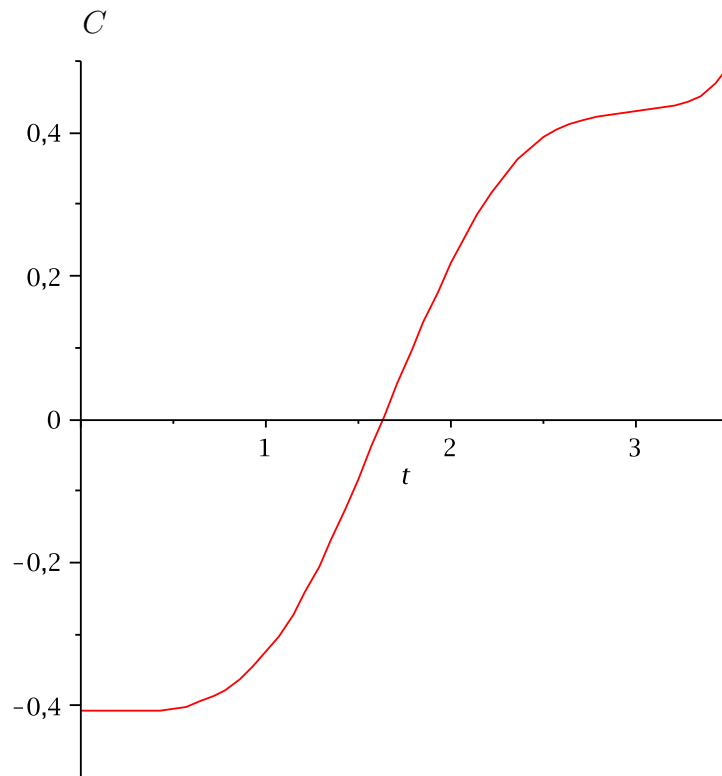


Figure 14: Shooting from the lower boundary: for $\bar{\Lambda} = 0.5$ and for $\kappa^2 = 0.640000$ (slightly bigger than the fine-tuned value), the function C is shown. The field C' never reaches the value $C' = 0$, therefore the field C never settles down at its vacuum value. The field $C(t)$ takes the value zero at $t = 1.63363$, which is markedly different from the point where the field ξ takes the value zero in Figure 13.

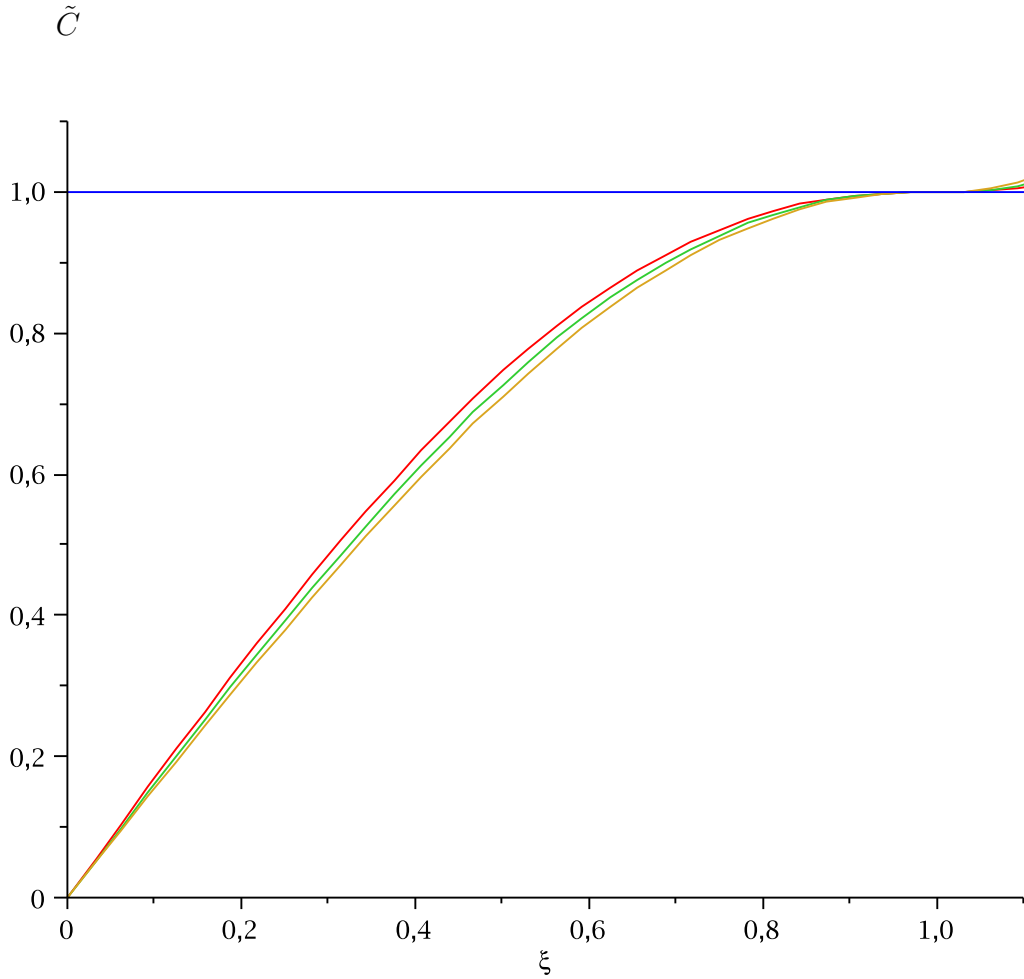


Figure 15: Integration of the orbit equation (39) for some fine-tuned values of κ and $\bar{\Lambda}$. The values of the parameters and the resulting $\tilde{C}(\xi = 1)$ are upper curve: $\bar{\Lambda} = 0.005$, $\kappa = 0.2303457790$, $\tilde{C}(\xi = 1) = 1.0000029$, middle curve: $\bar{\Lambda} = 1.5$, $\kappa = 1.119251347$, $\tilde{C}(\xi = 1) = 1.0000074$, lower curve: $\bar{\Lambda} = 6.0$, $\kappa = 1.818434381$, $\tilde{C}(\xi = 1) = 0.9999953$. So \tilde{C} reaches the compacton value $\tilde{C}(\xi = 1) = 1$ to a high precision.

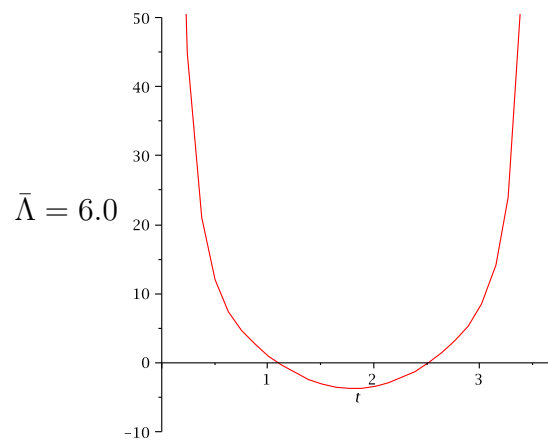
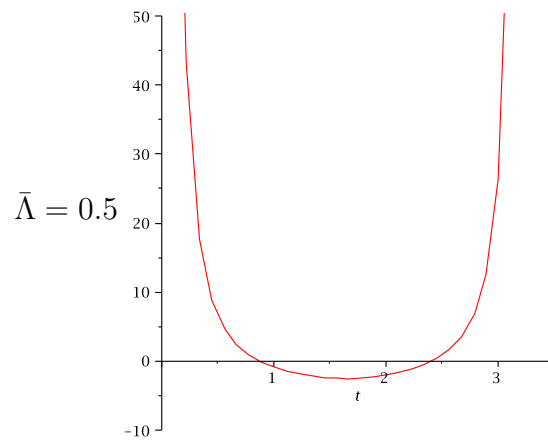
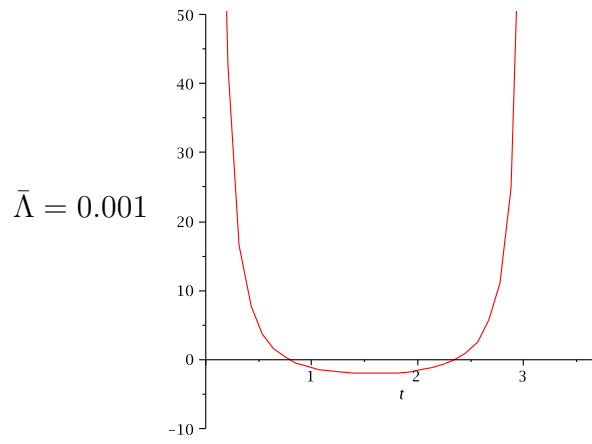


Figure 16: The potential U for the effective Schroedinger equation of Section 6, for the values $\bar{\Lambda} = 0.001, 0.5, 6.0$.

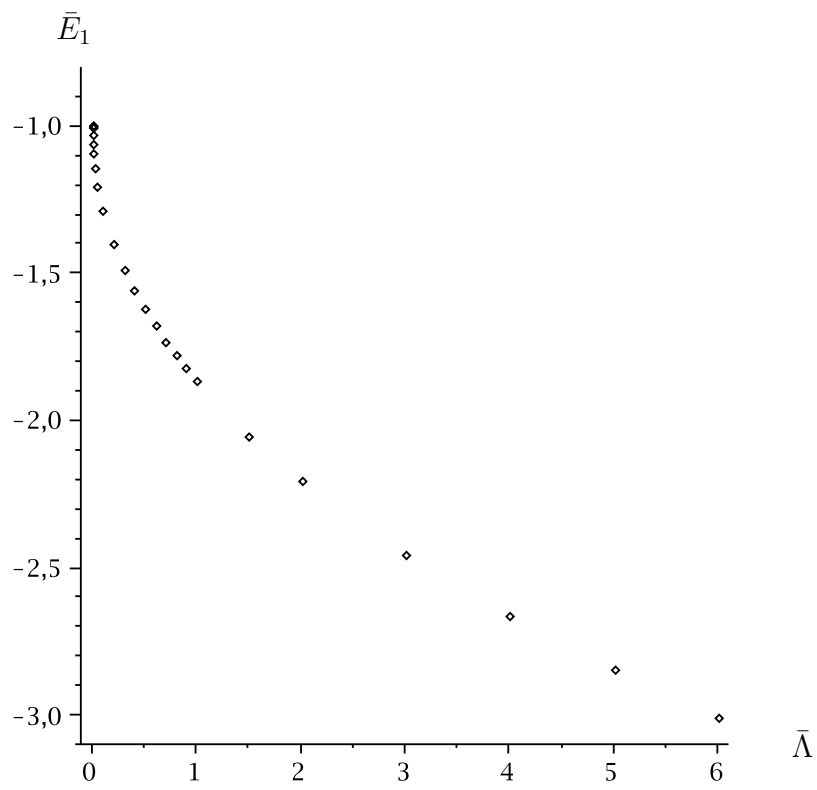


Figure 17: The first energy eigenvalue of the infinite square wall potential of Section 6. The eigenvalue is negative for all values of $\bar{\Lambda}$

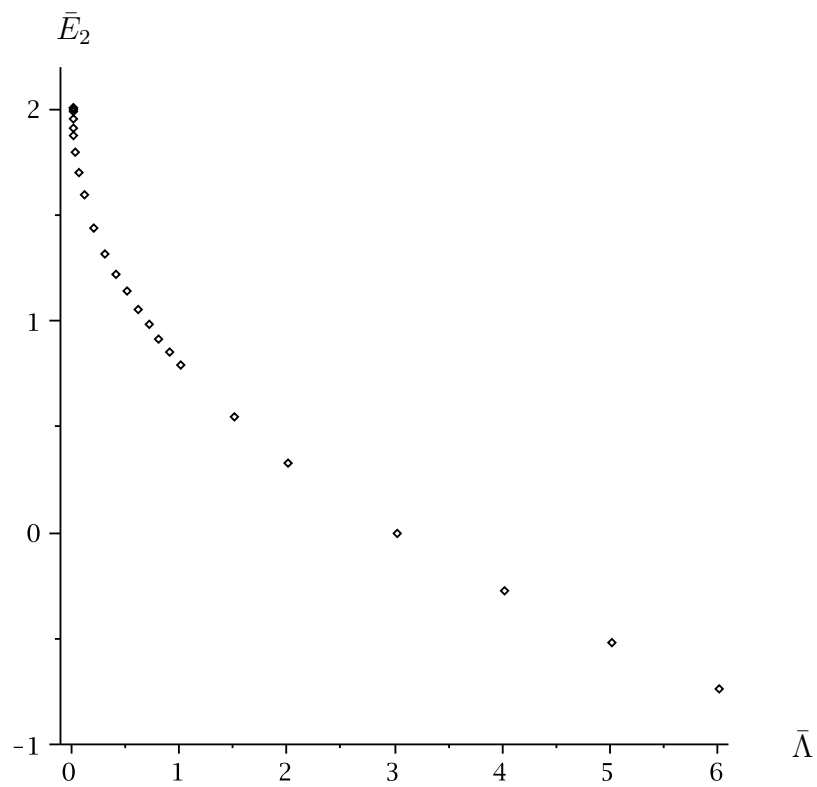


Figure 18: The second energy eigenvalue of the infinite square wall potential of Section 6. The eigenvalue is positive for sufficiently small values of $\bar{\Lambda}$ (at least till $\bar{\Lambda} = 2$)